Laser Assisted Cold Spray Deposition

Venkata Satish Bhattiprolu and Luke N. Brewer

Abstract This chapter will review the current state of the utilization of lasers to enhance the cold spray process both during and after deposition. While high and low-pressure cold spray has been successfully applied to a variety of metallic alloys, there is a need to increase deposition efficiency, permit the use of heavier and less expensive spray gases, and to tailor the microstructure of the sprayed material. Over the past decade, laser-assisted cold spray (LACS) has been introduced and developed to address these needs. In this process, the laser acts as a localized heat source softening the substrate and the deposited powder particles. This thermal softening in turn facilitates the deposition of hard materials and also enhances the deposition behaviour at lower powder particle velocities, allowing the use of less expensive processing gases like nitrogen. LACS has been applied in both co-axial and off-axis forms. The off-axis geometry has shown improvements in the deposition of titanium alloys, stellite, tungsten, and even oxide dispersion strengthened steel. While LACS can improve the deposition efficiency, it will also impact the microstructure of the sprayed material, either positively or negatively, depending upon the heat input used. Recent work has shown an increase in grain size and coarsening of precipitates during the LACS process. Understanding and controlling heat input during LACS are key to correctly producing the desired microstructure and mechanical properties of the deposited material. This chapter will introduce the LACS approach, present its applications to different alloy systems, discuss its advantages and disadvantages and offer some thoughts about its development in the near future.

Keywords Laser assisted cold spray · Supersonic laser deposition · Microstructure characterization · Mechanical properties

V. S. Bhattiprolu · L. N. Brewer (✉)
Department of Metallurgical and Materials Engineering, The University of Alabama, Box 870202, Tuscaloosa, AL 35487-0200, USA
e-mail: lnbrewer1@eng.ua.edu

S. Pathak and G. C. Saha (eds.), *Cold Spray in the Realm of Additive Manufacturing*, Materials Forming, Machining and Tribology,
https://doi.org/10.1007/978-3-030-42756-6_6

1 Motivation and Introduction

Cold spray (CS) is a solid-state deposition process involving severe plastic deformation of micron-sized powder particles (~40 μm) onto a metal substrate. The bonding of individual particles to the substrate is accomplished through metallurgical bonding and mechanical interlocking. The CS process has been successfully employed to produce dense coatings for a wide variety of materials as shown in Table 1. The coatings typically exhibit high hardness, compressive residual stresses, and high wear resistance [1]. In some cases, CS coatings demonstrate tensile strengths comparable to bulk materials (Table 1).

Most of the early cold spray research involved relatively "soft" materials like aluminum and copper. This emphasis was in large part due to their lower critical velocities. Assadi and Schmidt have developed the concept of critical velocity in which particles with a velocity higher than the critical velocity adhere to the substrate upon impact [23]. As shown in Eq. 1 [23], the critical velocity is directly proportional to the ultimate tensile strength of the material being sprayed. Soft powder materials such as copper, commercially pure aluminum, and nickel have a relatively low critical velocity and thus can be readily sprayed. "Hard" powder materials, such as alloyed aluminum, ferritic steels, titanium, and nickel-based alloys require higher particle velocities for successful deposition (i.e., owing to higher critical velocity). This increase in particle velocity can be achieved by higher gas pressure, higher gas temperature, or by the use of a lighter spray gas. The nozzle exit velocity for powder particles is directly proportional to the gas velocity which is in turn inversely proportional to the molecular weight of the gas being sprayed, as shown in Eq. 2.

Table 1 Representative characteristics for metallic deposits produced using high-pressure cold spray

CS Deposition property (as-sprayed)	Aluminum (Al) and aluminum alloys	Copper (Cu)	Austenitic Stainless Steel	Titanium (Ti) and titanium alloys
Porosity (area%)	0.25 (Helium) [2] 0.32 (Nitrogen) [2]	0.04 (Nitrogen) [3]	~1% (Helium) [4] ~2% (Nitrogen) [5]	~0.3% (Helium) [6] ~11% (Nitrogen) [7]
Microhardness	25–50% higher hardness than cold worked Al [1, 8]	20% higher hardness than annealed and cold rolled Cu (150 $HV_{0.3}$) [9]	157% higher than bulk SS substrate (410 $HV_{0.3}$) [10]	16% higher hardness than bulk Ti [11]
Tensile strength (MPa)	410–440 [12–14]	~140 to 300 [3, 15, 16]	~67 to 525 [4, 17, 18]	~445 [19]
Ductility (% Elongation) in as-sprayed condition	1–3.2 [12, 14, 20]	0.2–3 [3, 15, 16]	0.1–0.4 [3, 17, 18]	~0.45 to 3 [21, 22]

Table 2 Comparison of powder particle velocities and critical velocities for "soft" and "hard" powder types

Material type	Powder particle velocities (m/s)		Critical velocity of powder particles (m/s)
	Helium processing gas	Nitrogen processing gas	
CP Aluminum	1613	761	476
Ti6Al4V	1446	703	1103

These estimates were made using Eqs. 1 and 2. A powder particle diameter of 25 μm was assumed along with a particle temperature ~150 °C

Helium is the lightest gas commonly used for cold spray, and it readily accelerates powder particles to higher velocities resulting in a greater extent of plastic deformation of particles upon impact and in the dense deposited material. However, helium is expensive and as such cheaper alternatives (e.g. nitrogen) are increasingly sought for producing CS coatings. Table 2 provides typical powder particle velocities for commercially pure (CP) aluminum and Ti6Al4V using nitrogen and helium gases. It is apparent that the velocities of powder particles are higher than the critical velocity for CP aluminum even with nitrogen processing gas.

$$V_{critical} = \sqrt{\left(\frac{A\sigma}{\rho}\right) + BC_p(T_m - T)}; \tag{1}$$

where A, σ, ρ, B, C_p, T_m, T, denote a fitting constant, temperature-dependent flow stress, density, a second fitting constant, the heat capacity of the material, melting temperature, and powder particle temperature, respectively. Here the temperature-dependent flow stress of the material is assumed to be directly proportional to the ultimate tensile stress of the material [23].

$$V_g = \sqrt{\left(2\left(\frac{\gamma}{\gamma - 1}\right)\left(\frac{R}{M_{gas}}\right)T_g\left(1 - \left(\frac{p}{p_i}\right)^{\frac{\gamma-1}{\gamma}}\right) + V_{gi}^2\right)}: \tag{2}$$

where γ, p, R, M_{gas}, T_g, p_i, V_{gi}, denote specific heat ratio, gas pressure, the ideal gas law constant, the molecular weight of the gas, gas temperature, initial gas pressure, and initial gas velocity, respectively [24].

The main challenge with the mechanical properties of cold sprayed material is their low ductility in the as-sprayed condition (Table 1). Primarily due to the severe strain hardening of the powder particles during the CS process, the resultant coating is relatively brittle. It is however reported that post-spray annealing can recover the detrimental effects of strain hardening through static recovery and recrystallization [20]. Hall et al. sprayed commercially pure aluminum material using helium gas [20]. The resultant material had a UTS of ~140 to 195 MPa with an elongation to failure of only ~0.4 to 1% (Fig. 2) [20]. This material exhibited a very fine-grained microstructure, as is typical of a severely cold worked material (Fig. 1).

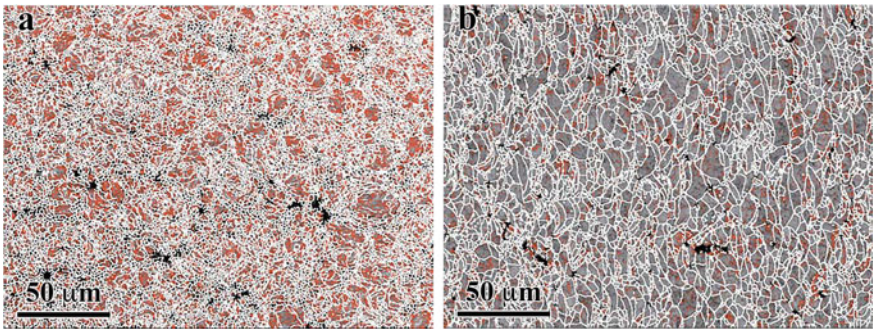

Fig. 1 Effect of annealing at 300 °C for 22 h on the microstructure of cold sprayed commercially pure aluminum. Microstructure evolved from **a** fine equiaxed grains before annealing to **b** coarse equiaxed grains after the annealing heat treatment (taken from Hall et al. [20])

After annealing at 300 °C for 22 h, the same CS coatings (Fig. 1b) possessed larger grains due to full recrystallization and subsequent grain growth. Unsurprisingly, the elongation to failure increased to 6–10% for the range of powders investigated, as shown in Fig. 2. A similar increase in the ductility and corresponding decrease in the tensile strength was observed by Coddett et al. for helium sprayed stainless steel 304 CS coatings after annealing [4]. The coatings exhibited tensile strengths of ~630 and ~425 MPa before and after annealing to 1050 °C for 4 h; the coatings exhibited ductilities of ~0 and 10% before and after annealing, respectively. Recently, however, Rokni, M. R. et al. reported an increase in both ductility and tensile strength of CS aluminum alloy Al 7075 with heat treatment [14]. These increases were attributed to the precipitation of intermetallic phases during heat treatment which subsequently hinders dislocation movement during tensile testing [14]. Accordingly, the relative increase in strength and ductility amounted to 19 and 138%, respectively. In the same work, it was reported that annealing CS Al 7075 to 412 °C for 3 h resulted in ductility of 14%, which corresponds to an increase of 338% from the as-sprayed condition [14].

In summary, the CS process has been consistently employed to deposit a range of metallic materials, but with challenges in terms of the gas required and the ductility of the as-sprayed material. The stronger the metallic material, the higher its critical velocity, necessitating higher spray gas pressures, higher spray gas temperatures, and the use of lighter spray gases. The use of helium gas has been quite successful, but it adds a high cost to the CS process. Post-spray annealing can expand the CS material selection and improve the material ductility, but these post-processing steps can quickly become financially unattractive, particularly for large parts. There is a need to balance the cost of the CS process with its mechanical properties for both soft and hard alloys. Laser-Assisted Cold Spray (LACS) is an exciting approach that builds on the cold spray process by adding in situ laser heating.

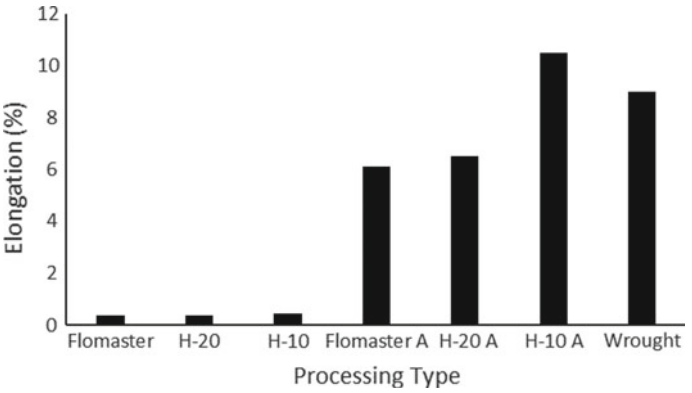

Fig. 2 Effect of annealing at 300 °C for 22 h on the ductility of CS depositions produced using Al powder procured from various suppliers (modified from Hall et al. [20]) and compared to wrought material. The letter A stands for annealed samples. The two labels Flomaster, and H, represent gas atomized aluminum powder procured from Valimet, and F. J. Brodman, respectively. The numbers 10 and 20 listed as a suffix to H indicate the average powder particle size of Valimet powder: 10 denoting ~12 μm and 20 denoting ~26 μm

2 Laser-Assisted Cold Spray (LACS) Deposition

The LACS process involves the employment of a laser along with the de Laval CS nozzle for enhancing the deformation of the substrate/deposited powder particles by softening them in situ. This process is also referred to as supersonic laser deposition in some of the related literature [25]. In addition, the in situ heating can also be used to modify the microstructure during LACS. Other work by Christoulis, D. and Sarafoglou, C. has used lasers to clean the substrate just prior to particle deposition, and while intriguing, it will not be reviewed in this chapter, but it is described in the book *Modern Cold Spray* [26]. A fair amount of work on the literature has also considered the use of post-spray laser heating. This related approach is not the focus of the current chapter, but it will be discussed in later sections.

To date, three different laser configurations have been investigated with respect to the de Laval CS nozzle: (1) Laser co-axial with the spray deposition, (2) Laser off-axis with the laser spot coincident with the centre of the spray deposition, and (3) Laser off-axis with the spray deposition, with the nozzle trailing the laser beam. The third configuration was utilized by the investigators to avoid melting of Al-12%Si powder particles if exposed directly to the laser beam [27]. Among the three configurations, the off-axis geometry with the laser and the spray nozzle coincident on the substrate has received the most attention in the literature. The experimental setup for these different configurations and the important properties of the produced coatings will be discussed in detail below.

2.1 Co-axial Laser Assistance (COLA) During CS

In the co-axial configuration, the laser beam is directed along the axis of the CS nozzle [28, 29]. The literature for COLA actually shows two different approaches. Figure 3a shows the COLA geometry used by Koivuluoto et al., in which multiple lasers are directed at a slight angle to the nozzle. These laser beams are *outside* of the spray nozzle but provide heat to a circular disc coincident with the spray [28]. Temperature sensors and a feedback control system change the laser power automatically during the LACS process as required [30]. Toom used an approach in which the laser beam is directed along the spray nozzle axis *from inside* the spray nozzle (Fig. 3b) [29]. The spray gas is introduced after the laser optics but prior to the converging section of the nozzle. The metal powder is injected after the throat into the diverging portion of the nozzle.

The coating characteristics are significantly affected by the introduction of a laser to the CS process. The coating density is shown to improve slightly with the assistance of a laser [28, 30]. In this regard, Koivuluoto et al. showed that the porosity decreased from 0.5 to 0.1% for a peak aged cold sprayed Al alloy coating with the employment of the laser [30]. Another related coating property, adhesion strength, was also reported to improve with LACS. This improvement via COLA was demonstrated for the

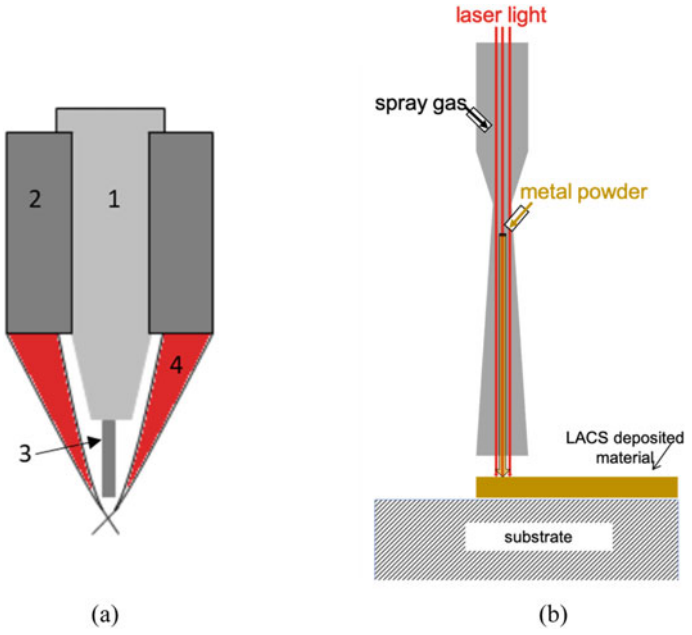

Fig. 3 Schematic of two geometries for the COLA Process: **a** (modified from Koivuluoto et al. [28]) where the numbers denote the following: 1. Spray Nozzle 2. Device for monitoring substrate temperature 3. Powder with gas and 4. Focused laser beams and **b** modified from Toom [29]

cold spray of Al, bronze alloys, Ni alloys, and Fe-Mn alloys by separate groups of investigators [29, 30]. Specifically, the adhesion strength increased from 27 to 48 MPa for cold sprayed aluminum with the employment of laser at a laser power of 1 kW [28]. Similarly, the adhesion strength increased from 27 MPa (regular CS) to 35 MPa (LACS) for Fe-Mn alloys with the internal COLA setup where the laser power was set to 200 W [29]. The laser is reported to promote substrate softening, which in turn results in better particle-particle bonding in the LACS coatings [28]. For these reasons, the cohesive strength of Cu bronze and Al alloy coatings was shown to be improved from 4 to 29 MPa and 119 to 177 MPa, respectively [30]. Koivulouto has proposed that the higher density and substrate-coating bond strength produced by the LACS process could provide enhanced barrier coatings for corrosion prevention on chemically active materials [28].

The in situ laser heating during co-axial LACS also affects the hardness of the deposited material. Due to softening of the substrate and the deposited powder particles during the LACS process, the hardness of LACS coatings is generally lower than for cold sprayed coatings [28, 30]. Again, hardness was shown to decrease from ~350–390 $HV_{0.1}$ to ~290–330 $HV_{0.1}$ for Cu bronze alloys with the application of a laser during CS. In the same study, the hardness decrease was 12–23% for COLA compared with CS of aluminum. This reduction in hardness is noteworthy as lower hardness may suggest better ductility of LACS coatings as compared to CS coatings.

2.2 Off-Axis Laser Assistance During CS

For most of the reported LACS literature, the laser is installed outside of and at an acute angle to the axis of the CS nozzle (Fig. 4). The laser's angle is adjusted in such a way that the focused laser spot is on the substrate and exactly below the CS nozzle, at a pre-determined standoff distance. An optical pyrometer is also often connected in parallel with the laser head. The temperature readings from the pyrometer can be used for substrate temperature control using a feedback control system, and thus the LACS experiment can be controlled according to laser power or measured surface temperature. In this configuration, the laser moves along with the nozzle during the spraying process.

One can estimate the amount of time that a particle in-flight interacts with the laser beam under the following assumptions based on typical CS conditions:

(1) the standoff distance between nozzle exit and substrate is 25 mm
(2) the laser spot diameter is 8 mm
(3) the average powder particle velocity is 800 m/s
(4) the CS nozzle and laser move at a velocity of 25 mm/s.

In this geometry, the amount of time a particle in flight is exposed to a moving laser beam is minuscule (~30 μs). Upon impact, the newly deposited particle will be irradiated for about 150 ms before it moves out of the laser spot diameter. Based on these estimates, the particle spends about 5000 times longer being irradiated after

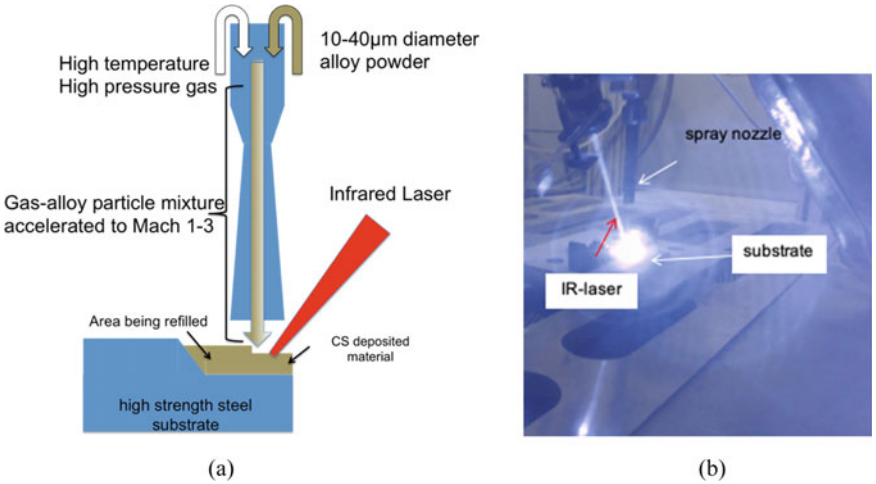

Fig. 4 The off-axis LACS process. **a** Schematic and **b** still-frame of video from LACS in operation at The University of Alabama

impact than during its flight to the substrate. This calculation strongly suggests that most of the thermal impact is from irradiation of deposited particles on the substrate, not from laser heating of the particles in flight. It should be noted that subsequent laser passes over deposited particles will continue to heat them.

The LACS process has been shown to improve the deposition efficiency of different materials. One of the earliest studies on the efficacy of the LACS process for improving the deposition behaviour of materials was reported by Bray et al. [31]. Bray et al. showed that the build rate of titanium powder increased two-fold from lower than 25 g/min to close to 45 g/min with the application of in situ laser heating [31]. Li, B. et al. reported a systematic increase in deposition efficiency with increasing surface temperature for LACS of Stellite-6 material (Fig. 5) [32]. The authors attributed this substantial increase in deposition efficiency to a decrease in the critical velocity of powder particles during impact due to an increase in powder particle temperatures (due to laser exposure). Kumala et al. made the interesting observation that deposition efficiency during LACS may be a coupled effect from both the surface temperature and the number of deposited layers (Fig. 6) [33]. For LACS of Cu+Al_2O_3 the impact of laser heating for only two deposited layers was minimal, while for ten deposited layers, laser heating clearly increased deposition efficiency [33]. This dependence upon layer thickness may be due to the cumulative heat input provided to the deposited material as the number of layers increases.

The LACS process has also been employed for the deposition of hard materials with good success. Several materials, including tungsten [34], Ni60 [35], Ni60-Diamond composite [36], tungsten carbide-stainless steel (W-SS) composite [37], and oxide dispersion strengthened steel (Fe-8Ni-1Zr) [38], have been successfully

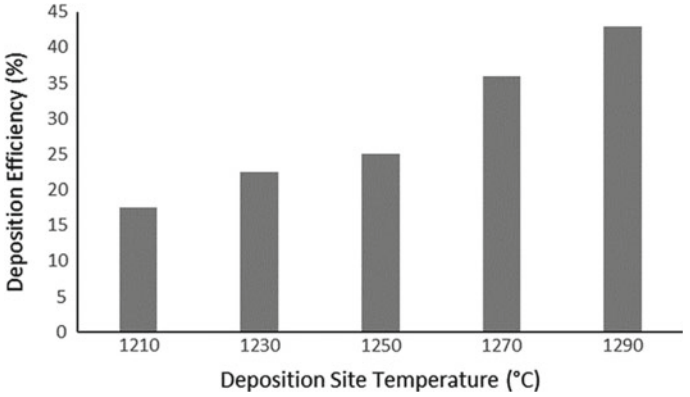

Fig. 5 DE of Stellite-6 depositions on medium carbon steel substrates at a maximum laser power of ~1.5 to 1.8 kW as a function of deposition temperature (modified from Li et al. [32])

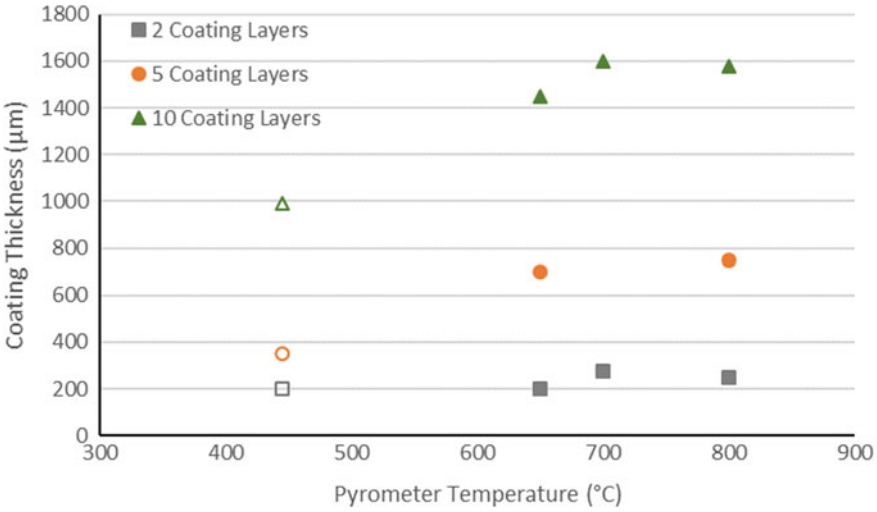

Fig. 6 Change in coating thickness as a function of both deposition temperature and a number of layers in Cu+Al_2O_3 cold sprayed depositions produced on low carbon steel using LACS with laser power between 1.8 and 2.4 kW. Here the open symbols represent the gas temperature for the CS depositions where the laser was not employed (i.e., regular CS) (modified from Kulmala et al. [33])

produced using the LACS process over the past five years. These results are significant, as producing these coatings using regular CS is very challenging. Li et al. [37] have demonstrated the effectiveness of LACS for challenging materials quite clearly with their recent work on WC-SS316L composite depositions. Without laser heating, CS was only able to produce coatings which retained a WC composite loading of 24% (Fig. 7). Note that the data point at a deposition temperature of 450 °C is for a regular CS process (i.e., without laser) where the temperature denotes the stagnation

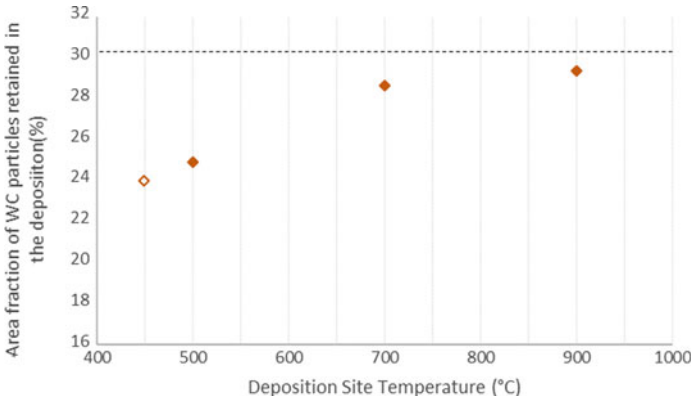

Fig. 7 Concentration of WC particles in the composite WC-SS LACS coatings produced using nitrogen gas on a SS substrate at different deposition site temperatures (modified from Li et al. [37]). Here, the deposition site temperature 450 °C represents gas temperature and this deposition was produced without a laser (i.e., regular CS). The dashed line represents the volume % of WC particles in WC-SS composite powder

gas temperature with the assumption that deposition temperature is the stagnation gas temperature (which is likely an overestimate) (Fig. 7). As seen, the area fraction of retained WC ceramic particles within the WC-SS316L composite increases systematically with an increase in the laser heat input. At a deposition site temperature of 950 °C (highest heat input), the area fraction of WC particles in the deposited material nearly matched the fraction of powder feedstock composite loading at 30% (Fig. 7). This increase in the ceramic concentration of the deposited composite material was attributed to increased embedment of WC particles, stemming from enhanced softening of the metal matrix at elevated deposition temperatures [37].

The potential for LACS to successfully produce materials based upon hard alloys is further illustrated from recent results on 4340 steel (Fig. 8). The 4340 steel material was deposited using helium processing gas (4.14 MPa and 550 °C) and a deposition site temperature of 950 °C by employing a 4 kW continuous diode laser. As observed in Fig. 8, the resultant coating was very dense with negligible (~0.1 area%) porosity and a deposition efficiency of 70%. This density is close to what is generally reported for soft materials like aluminum alloys using helium [1]. Figure 8 also shows evidence of CS tracks from multiple passes in the longitudinal direction. These tracks may be interfaces between layers of CS deposition and are typically not observed in CS coatings. Some oxidation of the steel surface between CS passes may be occurring at this elevated temperature.

LACS is also showing promise for the deposition of wear-resistant materials. Specifically, the wear resistance of LACS-produced material was compared to that from laser cladding, a widely used process for producing well-adhered [35] coatings for wear protection [39]. In general, LACS depositions were characterized by superior wear properties (i.e., lower coefficient of friction, lower volume loss, and lower depth of wear track) when compared to laser clad materials. This improvement was mainly

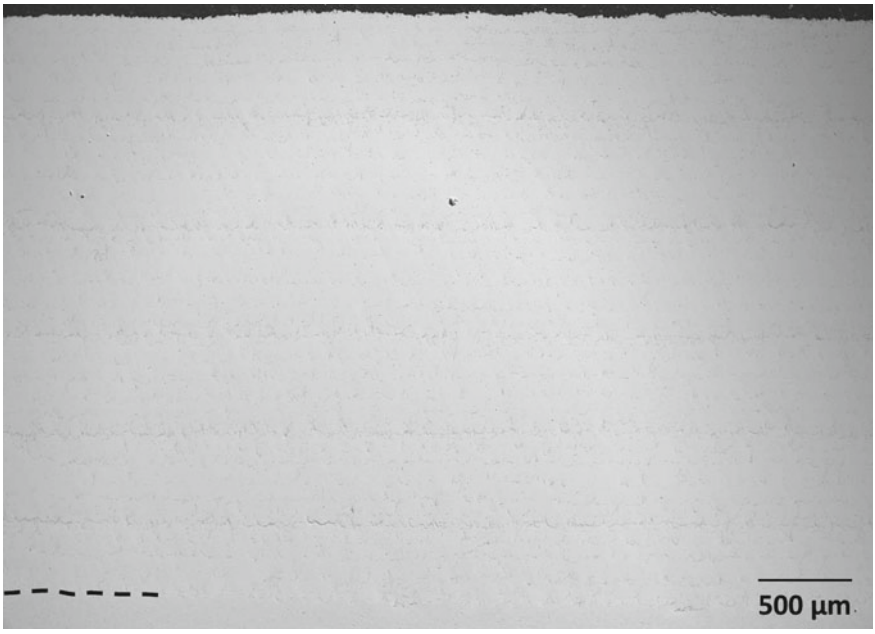

Fig. 8 Low magnification back scatter electron image of 4340 Steel deposited using the laser assisted cold spray process. The black dashed line represents approximate location of interface between coating (top) and the substrate (bottom)

attributed to lower heat input and to a finer microstructure in the LACS process when compared to laser cladding. In addition, LACS did not alter the phases present in the material before and after deposition.

The LACS process may also allow for the deposition of both soft and hard materials (especially titanium alloys) using nitrogen as the spray gas. As nitrogen is significantly less expensive than helium as a spray gas, the ability to still efficiently deposit high-quality material using LACS with nitrogen as the spray gas is a significant development. Evidence for producing dense LACS coatings using nitrogen gas is readily apparent from Table 3 for different material systems.

The LACS process produces characteristically different microstructures when compared to regular CS, especially when considering the prior-particle morphology. This change is clearly shown in Fig. 9, for a titanium coating produced by LACS at a deposition site temperature of 500 °C [31]. Starting with spherical titanium powder particles, the LACS process produced a coating microstructure with relatively equiaxed prior-particle morphologies, particularly at the bottom of the coating. In regular CS, the prior-particles are often much flatter (high aspect ratio) due to repeated peening by subsequent particles during the deposition. Similar results have been recently observed for LACS of 4340 steel, particularly at higher deposition temperatures. The reasons for this change in prior-particle morphology between CS and LACS is still an open question.

Table 3 Table demonstrating the laser parameters and deposition properties for various LACS depositions using nitrogen as the spray gas

	CP aluminum (Al)/Al alloys	Tungsten	Stellite-6	CP Ti/Ti6Al4V
Laser power	Al-12%Si: 2.5 kW [27]	4 kW [34]	1.5 kW [32, 40]	Ti6Al4V: 300 W to 1 kW [41] CP Ti: 650 W-1 kW [31]
Deposition surface temperature	CP Al: 450 °C [42] Al-12%Si: 200 °C [27]	Outside the range of pyrometer [34]	1210–1290 °C [43]	≤900 °C [41] CP Ti: 450–900 °C [31]
Substrate	Al-12%Si: Stainless Steel 304 [27] CP Al: Stainless Steel 304 [42]	Molybdenum [34]	Medium carbon steel [43]	Ti6Al4V: Ti6Al4V [41] CP Ti: Low carbon steel [25]
Gas	Al-12%Si: N_2 [27] CP Al: N_2 [42]	N_2 [34]	N_2 [43]	Ti6Al4V: N_2 [41] CP Ti: N_2 [31]
Porosity (area%)	Al-12%Si: 0.16 [27] CP Al: 0.01–0.04 [42]	5 [34]	NR	Ti6Al4V: 0.1 [41]
Hardness	CP Al: 46–51 $HV_{0.05}$ [42]	NR	693 $HV_{0.2}$ [43]	Ti6Al4V: Min of 331 $HV_{0.2}$ and Max of 461 $HV_{0.2}$ [41] CP Ti: 272 $HV_{0.3}$ [25]
Adhesion strength	NR	NR	NR	CP Ti: 77 MPa [25]
Tensile strength	NR	725 MPa [34]	718.3 MPa [43]	NR

Some values were not reported in the literature and thus designated by "NR"

The high temperatures during LACS can also result in an in situ, static recrystallization of the deposition microstructure, as seen from Fig. 10. This figure depicts feedstock Ti6Al4V powder characterized by a martensitic alpha grain microstructure. This microstructure evolves during LACS to a microstructure comprised of equiaxed alpha grains due to recrystallization. This substantial change in the microstructure was ascribed to high laser power and low raster speed of the CS nozzle [41]. Heat input during LACS can also result in grain growth during the deposition process (Fig. 11). In this figure, the microstructural characteristics of cold sprayed Fe-8Ni-1Zr oxide dispersion strengthened (ODS) steel depositions with and without in situ laser heating were captured using electron backscatter diffraction (EBSD) and 3D

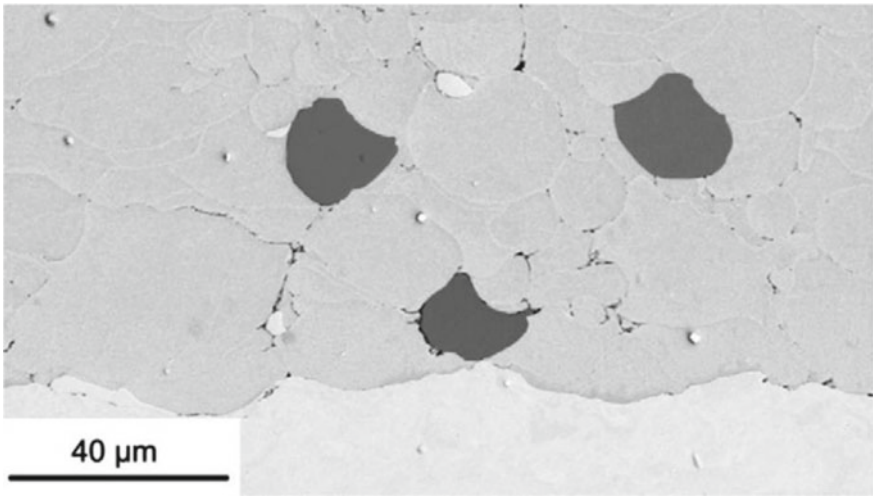

Fig. 9 Deformed particles within LACS deposition of titanium at deposition surface temperature of 500 °C (taken from Bray et al. [31]). Here, the three particles with dark contrast were shaded post-deposition to highlight the unique morphology of LACS particles

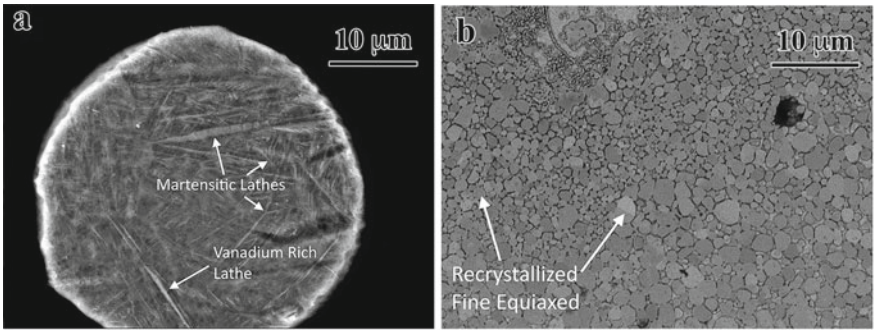

Fig. 10 **a** As-received Ti-6Al-4V powder martensitic microstructure and **b** recrystallized microstructure within Ti-6Al-4V LACS deposition at laser power of 600 W (taken from Birt et al. [41])

atom probe tomography [38]. An apparent increase in the grain size (~300%) was observed as the deposition site temperature increased from 320 °C in CS-only to 950 °C in LACS [38]. Further, the non-uniform grain growth observed at the highest LACS deposition temperature (950 °C) was attributed to abnormal grain growth due to the presence of nanoscale oxide dispersants [38]. Furthermore, a 36% reduction in microhardness was reported with the LACS process and was partially ascribed to the observed grain growth [38]. Interestingly, the nanoscale oxide particles survived the LACS process, even at 950 °C, and coarsened only slightly from an inter-particle spacing of 17 nm for CS-only to 23 nm at 950 °C [38].

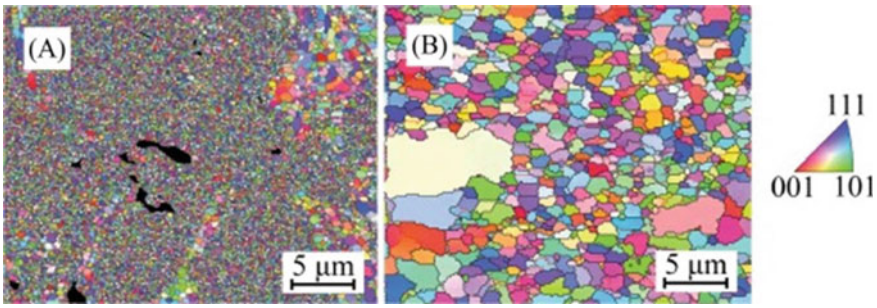

Fig. 11 **a** EBSD orientation map of Fe-8Ni-1Zr ODS deposition without laser heating at deposition site temperature of 320 °C, **b** EBSD micrograph of Fe-8Ni-1Zr ODS deposition with laser heating at a deposition site temperature of 950 °C (taken from Story et al. [38])

The evidence of recrystallization and grain growth during the LACS process suggests that an increase in ductility for as-sprayed material may be possible. Several studies of materials produced with LACS have shown recrystallized microstructures with a correlated reduction in hardness. Actual measurements of ductility for LACS deposited material are scant in the current scientific literature, however, recent results on LACS of AA7075 powders demonstrate increases in ductility [44]. As-atomized AA7075 powder was sprayed using helium gas both with and without a 1.6 kW laser (940 nm wavelength, spot size 8 mm) [44]. The cold sprayed material showed elongation to failure values of $0.7 \pm 0.07\%$ as-sprayed, while the LACS-deposited material exhibited increased elongation to failure to $2.1 \pm 0.3\%$ in the as-sprayed condition [44]. The maximum stress prior to fracture showed the opposite behaviour: CS material had maximum stress of approximately 360 MPa, while the LACS-deposited material exhibited maximum stress of approximately 320 MPa [44].

2.3 Laser Heating Post Cold Spray (LHCS)

Laser heat treatment can also be employed after the cold spray process. These post-deposition heat treatments have been applied as both surface re-melting and as solid-state annealing of the cold sprayed coating. [45–47]. Work by Marrocco, T. et al. involved re-melting of CS deposited CP titanium using a 2 kW CO_2 laser [45]. Similarly, work reported by Poza, P. et al. involved re-melting of Inconel 625 CS coatings using a 1.3 kW diode laser [47]. The high laser powers resulted in melting followed by pore closure due to diffusion of material to high energy surfaces. This reduction in porosity, in turn, was reported to improve the corrosion resistance of the CS coatings [45, 46] and in one case the laser re-melted material reached the properties of bulk material [45]. In addition to pore reduction, the prior-particle interfaces generally seen in CS coatings were also reported to disappear with the laser re-melting [45]. While laser post-heating has a beneficial impact on the surface

of the CS coating, it could also affect the substrate in some cases. This substrate impact can be expected at a high linear heat input (either from high laser power or slow nozzle raster speed or a combination of both) [47]. Additionally, due to the large thermal gradient between the re-melted region near the surface and the region near the substrate-coating interface, tensile residual stresses may be present in the LHCS coatings. Their presence could be detrimental to the properties of the LHCS coating.

The amount of heat input during the laser re-melting process is also reported to affect the quality of the coating significantly. Whereas a low heat input may not result in a visible change, high heat input can cause cracks in the coating [48, 49]. Additionally, it is shown to stratify the CS deposition by forming three zones with three different microstructures: (1) re-melted zone (2) heat affected zone and (3) base material [49]. Among these regions, the re-melted zone is reported to exhibit a rapidly solidified microstructure with high hardness [49].

LHCS has also been recently investigated for post-cold spray solid-state annealing [50]. Four material systems were investigated; Aluminum alloy 6061 (AA 6061), Copper (Cu), SS 304, and Grade 2 Titanium (Ti). Among these materials, it was reported that only Al 6061 and Cu exhibited a reduction in hardness. This may be due to the low laser power utilized (i.e., 95 W). Interestingly, Aldwell, B. et al. also reported cracking of the SS deposits with LHCS after 10 laser passes and hypothesized that it might be due to thermal cycling [50]. This result is similar to what has been observed by a separate group of researchers for grade 2 titanium, as mentioned previously [48].

In summary, LHCS of materials has significant potential for reducing porosity, reducing the detrimental effects of strain hardening, and for improving the corrosion resistance of the CS deposition. With further work on optimization of laser parameters, it is expected that the detrimental effects of laser heating on CS materials may be mitigated (e.g., tensile residual stresses and cracks). Although, not currently reported, LHCS of certain materials (e.g., SS 304) may also result in grain boundary sensitization, especially at the high deposition site temperatures of the laser. Thus, along with mitigating residual stresses, further work on laser parameter optimization may be needed for prevention of sensitization (on susceptible materials).

3 Advantages, Disadvantages, and Directions for the Future Development of the LACS Process

The key advantage of the LACS process is its ability to provide a controlled amount of heating during the cold spray process. This laser heating can reduce the critical velocity of metallic powder particles during cold spray, ostensibly by softening the substrate and the deposited material. This reduction in critical velocity potentially allows the use of heavier, and usually, less expensive gases for LACS deposition. This benefit has already been well demonstrated for the LACS deposition of titanium [31].

In addition, "harder" metallic materials can be deposited by LACS than is possible from CS alone. This chapter has shown that a variety of difficult materials are now successfully sprayed with LACS, including Stellite, WC-stainless steel composites, ODS steel, and 4340 steel. The laser heating can also cause in situ recrystallization potentially increasing the ductility of the as-sprayed material. Finally, the amount of control from laser heating is potentially very good. The amount of laser power can be varied during the spray to achieve the desired microstructure at different locations in the deposition. It is also possible that lasers could be used for localized in situ heating in the field repair applications on structures far too large to be placed into a furnace.

The potential disadvantages of the LACS process are primarily those associated with increased thermal input. The key advantages of CS with respect to thermal spray techniques are primarily related to its low thermal input. The thermal impact of LACS is between CS and thermal spray. With excessive heat input, LACS may damage substrates under thin depositions; the thermal loading on the substrate will have to be carefully monitored and controlled, particularly in repair applications. LACS and LHCS may lead to unwanted oxide formation. While LACS may lead to increased ductility, it can also produce more softening than desired through the dissolution of precipitates, the recovery of dislocation structures, and due to excessive grain growth. In addition, LACS will produce much larger thermal gradients than CS, potentially resulting in tensile residual stresses in the deposited materials. Management of the residual thermal stresses produced by LACS will be necessary for mechanical reliability of these materials. Lastly, LACS requires the purchase and use of laser systems which add to the cost and complexity of the CS system, although the laser systems are typically less than half of the cost of the CS system itself.

LACS has shown great potential but still has several avenues which need to be explored and developed. The measurement, control, and optimization of heat input are the most important of these topics. The substrate and the newly deposited material are clearly heated by the in situ lasers, but there are other meaningful sources of heat including the heat from the CS gun itself and from subsequent passes of the laser/CS spray gun. In recent work on LACS of 4340 steel, CS conditions of 550 °C and 4.14 MPa using helium gas, resulting in a surface temperature without the laser of approximately 400 °C. Development of appropriate simulation tools will significantly aid in understanding and predicting the evolution of temperature in the substrate and the deposit during the LACS process. The raster pattern during LACS could also have more importance than in CS alone due to the potential of generating large thermal gradients and resultant residual stresses.

The interplay between thermal management and residual stresses is illustrated by recent work on LACS of 304 stainless steel (SS304) (Fig. 12). Initial LACS deposition of SS304 powder onto a SS304 substrate resulted in cracking of the deposited due to the large thermal gradients generated by the laser heating (Fig. 12a). The thermal conductivity of SS304 is particularly low and its thermal expansion coefficient is quite high, resulting in large thermal gradients and tensile residual stresses. The thermal gradients can be minimized by preheating the substrate with the laser immediately prior to LACS process. Figure 12b demonstrates the LACS SS304 coating produced

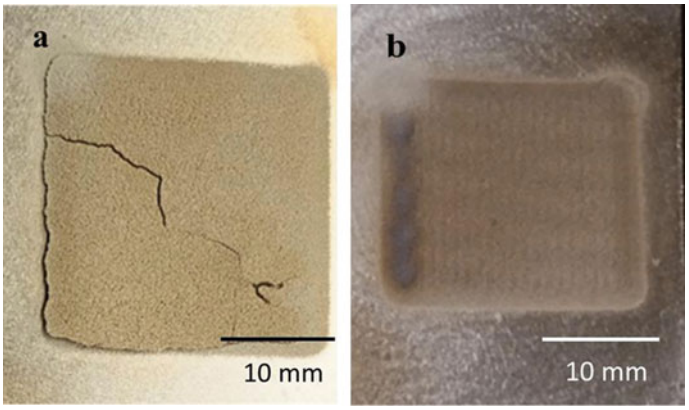

Fig. 12 SS 304 deposit produced by the LACS process **a** without laser heating the substrate prior to the process and **b** with heating the substrate prior to the process

with this laser pre-heating of the substrate. The reduced thermal gradient resulted in a successful deposition without any cracks. Because lasers can be precisely controlled, thermal cycles could be developed that can minimize residual stresses in the deposited material and substrate.

4 Conclusions

The laser-assisted cold spray (LACS) process combines the solid-state cold spray (CS) process with an in situ laser heating to lower the critical velocity required, to enhance material deposition efficiency, to evolve the microstructure during deposition, and to improve mechanical properties. LACS is performed using standard CS instruments modified with commercially available lasers, either co-axially with the spray nozzle or at an acute angle to the spray nozzle. LACS has been shown to enhance the deposition efficiency of materials that can be deposited by CS, including aluminum alloys, copper alloys, and titanium alloys. For titanium alloys, LACS allows the use of heavier, and less expensive, nitrogen gas while maintaining, and even improving the deposition efficiency as compared with CS alone. LACS has also been successfully used to deposit materials which cannot be successfully deposited by CS alone, including Stellite, high strength steels, tungsten, and even oxide dispersion strengthened alloys.

LACS has a number of advantages, disadvantages, and opportunities for future development. The key advantage of the LACS process is its ability to provide a controlled amount of heating during the cold spray process. This laser heating can reduce the critical velocity of metallic powder particles during cold spray allowing the use of heavier and less expensive gases for LACS deposition. In addition, "harder" metallic materials can be deposited by LACS than is possible from CS alone. The heat

input during LACS must be carefully managed or it may damage the substrate under thin depositions and cause unwanted oxide formation. The control and prediction of heat input is a crucial topic in the future development of LACS. A related need for further development is in the control and mitigation of residual stresses.

Acknowledgements The authors are very grateful for funding to support our research into LACS from the following sources: Office of Naval Research: (Dr. J. Wolk, AMMP N000141812266, Dr. A. Rahman, SBA N00014-18-1-2519, and Mr. W. Nickerson, DURIP N00014-16-1-2576) and the U.S. Department of Energy NEUP (18-15372 Workscope FC-4.2; Contract DE-NE0008770). In addition, we would like to thank J. Colburn, W. Compton, W. Story, and D. Barton for their assistance with the measurements from the UA Cold Spray Laboratory.

References

1. Champagne, V., & Helfritch, D. (2016). The unique abilities of cold spray deposition. *International Materials Reviews, 61*(7), 437–455.
2. Sharma, M. M., Eden, T. J., & Golesich, B. T. (2015). Effect of surface preparation on the microstructure, adhesion, and tensile properties of cold-sprayed aluminum coatings on AA2024 substrates. *Journal of Thermal Spray Technology, 24*(3), 410–422.
3. Huang, R., et al. (2015). The effects of heat treatment on the mechanical properties of cold-sprayed coatings. *Surface & Coatings Technology, 261,* 278–288.
4. Coddet, P., et al. (2015). Mechanical properties of thick 304L stainless steel deposits processed by He cold spray. *Surface & Coatings Technology, 277,* 74–80.
5. Dikici, B., et al. (2016). The effect of post-heat treatment on microstructure of 316L cold-sprayed coatings and their corrosion performance. *Journal of Thermal Spray Technology, 25*(4), 704–714.
6. Bhattiprolu, V. S., et al. (2018). Influence of feedstock powder and cold spray processing parameters on microstructure and mechanical properties of Ti-6Al-4V cold spray depositions. *Surface & Coatings Technology, 335,* 1–12.
7. Birt, A., et al. (2015). Microstructural analysis of cold-sprayed Ti-6Al-4V at the micro- and nano-scale. *Journal of Thermal Spray Technology, 24*(7), 1277–1288.
8. Champagne, V. K., et al. (2010). The effect of cold spray impact velocity on deposit hardness. *Modelling and Simulation in Materials Science and Engineering, 18*(6), 065011.
9. Stoltenhoff, T., et al. (2006). Microstructures and key properties of cold-sprayed and thermally sprayed copper coatings. *Surface & Coatings Technology, 200*(16–17), 4947–4960.
10. Huang, J., et al. (2019). Influence of cold gas spray processing conditions on the properties of 316L stainless steel coatings. *Surface Engineering*, 1–8.
11. Hussain, T. (2013). Cold spraying of titanium: A review of bonding mechanisms, microstructure and properties. In *Key engineering materials*. Trans Tech Publications Ltd.
12. Li, W., et al. (2018). Solid-state additive manufacturing and repairing by cold spraying: A review. *Journal of Materials Science and Technology, 34*(3), 440–457.
13. Rokni, M., et al. (2017). Microstructure and mechanical properties of cold sprayed 6061 Al in As-sprayed and heat treated condition. *Surface & Coatings Technology, 309,* 641–650.
14. Rokni, M., et al. (2017). The effects of heat treatment on 7075 Al cold spray deposits. *Surface & Coatings Technology, 310,* 278–285.
15. Yu, B., et al. (2019). Microstructural and bulk properties evolution of cold-sprayed copper coatings after low temperature annealing. *Materialia, 7,* 100356.
16. Yin, S., et al. (2018). Microstructure and mechanical anisotropy of additively manufactured cold spray copper deposits. *Materials Science and Engineering A, 734,* 67–76.

17. Meng, X.-M., et al. (2011). Influence of annealing treatment on the microstructure and mechanical performance of cold sprayed 304 stainless steel coating. *Applied Surface Science, 258*(2), 700–704.
18. Yin, S., et al. (2019). Annealing strategies for enhancing mechanical properties of additively manufactured 316L stainless steel deposited by cold spray. *Surface & Coatings Technology, 370,* 353–361.
19. Vo, P., et al. (2013). Mechanical and microstructural characterization of cold-sprayed Ti-6Al-4V after heat treatment. *Journal of Thermal Spray Technology, 22*(6), 954–964.
20. Hall, A. C., et al. (2006). The effect of a simple annealing heat treatment on the mechanical properties of cold-sprayed aluminum. *Journal of Thermal Spray Technology, 15*(2), 233–238.
21. Chen, C., et al. (2019). Effect of hot isostatic pressing (HIP) on microstructure and mechanical properties of Ti6Al4V alloy fabricated by cold spray additive manufacturing. *Additive Manufacturing, 27,* 595–605.
22. Zhao, Z., et al. (2019). Microstructural evolutions and mechanical characteristics of Ti/steel clad plates fabricated through cold spray additive manufacturing followed by hot-rolling and annealing. *Materials & Design*, 108249.
23. Schmidt, T., et al. (2009). From particle acceleration to impact and bonding in cold spraying. *Journal of Thermal Spray Technology, 18*(5–6), 794.
24. Champagne, V. K. (2007). *The cold spray materials deposition process*. Elsevier.
25. Lupoi, R., et al. (2011). High speed titanium coatings by supersonic laser deposition. *Materials Letters, 65*(21–22), 3205–3207.
26. Villafuerte, J. (2015). *Modern cold spray: Materials, process, and applications*. Berlin: Springer.
27. Olakanmi, E., et al. (2013). Deposition mechanism and microstructure of laser-assisted cold-sprayed (LACS) Al-12 wt.% Si coatings: Effects of laser power. *JOM, 65*(6), 776–783.
28. Koivuluoto, H., et al. (2017). Structures and properties of laser-assisted cold-sprayed aluminum coatings. In *Materials science forum*. Trans Tech Publications Ltd.
29. Reddy, S. (2017). Development of Fe-Mn alloy coatings using Coaxial laser assisted cold spray process. In *Mechanical engineering* (p. 69). Dearborn: University of Michigan.
30. Koivuluoto, H., et al. (2015). A novel coaxially laser-assisted (COLA) cold spray system. In *ITSC 2015-International Thermal Spray Conference*. Long Beach: ASM International.
31. Bray, M., Cockburn, A., & O'Neill, W. (2009). The laser-assisted cold spray process and deposit characterisation. *Surface & Coatings Technology, 203*(19), 2851–2857.
32. Li, B., et al. (2018). Influence of laser irradiation on deposition characteristics of cold sprayed Stellite-6 coatings. *Optics & Laser Technology, 100,* 27–39.
33. Kulmala, M., & Vuoristo, P. (2008). Influence of process conditions in laser-assisted low-pressure cold spraying. *Surface & Coatings Technology, 202*(18), 4503–4508.
34. Jones, M., et al. (2014). Solid-state manufacturing of tungsten deposits onto molybdenum substrates with supersonic laser deposition. *Materials Letters, 134,* 295–297.
35. Yao, J., et al. (2015). Characteristics and performance of hard Ni60 alloy coating produced with supersonic laser deposition technique. *Materials and Design, 83,* 26–35.
36. Yao, J., et al. (2015). Beneficial effects of laser irradiation on the deposition process of diamond/Ni60 composite coating with cold spray. *Applied Surface Science, 330,* 300–308.
37. Li, B., et al. (2015). Microstructure and tribological performance of tungsten carbide reinforced stainless steel composite coatings by supersonic laser deposition. *Surface & Coatings Technology, 275,* 58–68.
38. Story, W. A., et al. (2018). Laser assisted cold spray of Fe-Ni-Zr oxide dispersion strengthened steel. *Materialia, 3,* 239–242.
39. Vilar, R. (1999). Laser cladding. *Journal of Laser Applications, 11*(2), 64–79.
40. Luo, F., et al. (2012). Performance comparison of Stellite 6® deposited on steel using supersonic laser deposition and laser cladding. *Surface & Coatings Technology, 212,* 119–127.
41. Birt, A. M., et al. (2017). Statistically guided development of laser-assisted cold spray for microstructural control of Ti-6Al-4V. *Metallurgical and Materials Transactions A, 48*(4), 1931–1943.

42. Olakanmi, E. (2016). Optimization of the quality characteristics of laser-assisted cold-sprayed (LACS) aluminum coatings with Taguchi design of experiments (DOE). *Materials and Manufacturing Processes, 31*(11), 1490–1499.
43. Yao, J., et al. (2016). Characteristics and bonding behavior of Stellite 6 alloy coating processed with supersonic laser deposition. *Journal of Alloys and Compounds, 661,* 526–534.
44. Story, W. A. (2018). *Processing-microstructure-property relations in high pressure cold spray of AA2024 and AA7075*. University of Alabama Libraries.
45. Marrocco, T., et al. (2011). Corrosion performance of laser posttreated cold sprayed titanium coatings. *Journal of Thermal Spray Technology, 20*(4), 909.
46. Sova, A., et al. (2013). Cold spray deposition of 316L stainless steel coatings on aluminium surface with following laser post-treatment. *Surface & Coatings Technology, 235,* 283–289.
47. Poza, P., et al. (2014). Mechanical properties of Inconel 625 cold-sprayed coatings after laser remelting. Depth sensing indentation analysis. *Surface and Coatings Technology, 243,* 51–57.
48. Carlone, P., et al. (2016). Selective laser treatment on cold-sprayed titanium coatings: Numerical modeling and experimental analysis. *Metallurgical and Materials Transactions B, 47*(6), 3310–3317.
49. Astarita, A., et al. (2015). Study of the laser remelting of a cold sprayed titanium layer. *Procedia CIRP, 33,* 452–457.
50. Aldwell, B., et al. (2018). Fundamental investigation into the effects of in-process heat treatment in cold spray. In *ITSC 2018-International Thermal Spray Conference*. Orlando: ASM International.